

Hai-Jun Su

e-mail: suh@eng.uci.edu

J. Michael McCarthy

e-mail: jmmccart@uci.edu

Department of Mechanical and Aerospace  
Engineering,  
University of California, Irvine,  
Irvine, CA 92697

Layne T. Watson

e-mail: ltw@cs.vt.edu

Departments of Computer Science and  
Mathematics,  
Virginia Polytechnic Institute and State  
University,  
Blacksburg, VA 24061

# Generalized Linear Product Homotopy Algorithms and the Computation of Reachable Surfaces

*In this paper, we apply a homotopy algorithm to the problem of finding points in a moving body that lie on specific algebraic surfaces for a given set of spatial configurations of the body. This problem is a generalization of Burmester's determination of points in a body that lie on a circle for five planar positions. We focus on seven surfaces that we term "reachable" because they correspond to serial chains with two degree-of-freedom positioning structures combined with a three degree-of-freedom spherical wrist. A homotopy algorithm based on generalized linear products is used to provide a convenient estimate of the number of solutions of these polynomial systems. A parallelized version of this algorithm was then used to numerically determine all of the solutions.*

[DOI: 10.1115/1.1760550]

## 1 Introduction

The problem that we consider originates with the determination by Burmester [1] of those points in a body that lie on a circle for a given set of five planar positions. He used these so-called *Burmester points* to design a linkage to guide a body through the given positions. His result was a graphical solution to a set of five quadratic equations in five unknown parameters, see [2–4].

Chen and Roth [5] generalized this problem by seeking points and lines in a moving body that take positions on surfaces associated with articulated serial chains, in order to design robot manipulators. A subset of these serial chains consists of two joints that support a spherical wrist, and we consider the surfaces that are reachable by the wrist center of these chains. Considering the various ways of assembling these articulated chains, we obtain seven reachable algebraic surfaces. The equations of these surfaces can be evaluated on the displacement positions of a generic point in order to define a set of polynomial equations. The solution of these equations define the surface and the dimensions of the associated chains that guide the end-effector through the given displacements.

To illustrate this problem, consider the set of points,  $\mathbf{P}^i = (X_i, Y_i, Z_i)^T$ ,  $i = 1, \dots, n$ , that are the images of a point  $\mathbf{p} = (x, y, z)^T$  in a moving body defined by a set of spatial displacements  $T_i = [A_i, \mathbf{d}_i]$   $i = 1, \dots, n$ , which means  $\mathbf{P}^i = [A_i]\mathbf{p} + \mathbf{d}_i$ —note  $[A_i]$  is a  $3 \times 3$  rotation matrix and  $\mathbf{d}_i$  is a  $3 \times 1$  translation vector [6,7]. We now ask if there is a point  $\mathbf{p}$  in the moving body that has the property that the image points  $\mathbf{P}^i$  lie on a sphere, such that

$$(\mathbf{P}^i - \mathbf{B})^2 - R^2 = 0, \quad i = 1, \dots, n, \quad (1)$$

where  $R$  is the radius of the sphere and  $\mathbf{B} = (u, v, w)$  is its center. This sphere is defined by the seven parameters  $\mathbf{p} = (x, y, z)$ ,  $\mathbf{B} = (u, v, w)$  and  $R$ . Thus  $n = 7$  spatial displacements yield seven quadratic polynomials Eq. (1) that determine these parameters. The system of polynomials has a total degree of  $2^7 = 128$ , but it is known to have only 20 solutions [5,8].

Contributed by the Computer-Aided Product Development (CAPD) Committee for publication in the JOURNAL OF COMPUTING AND INFORMATION SCIENCE IN ENGINEERING. Manuscript received September 2003; Revised April 2004. Associate Editor: K. Lee.

In what follows, we study the cases of the plane, sphere, circular cylinder, circular hyperboloid, elliptic cylinder, circular torus and general torus (Fig. 1). These are the surfaces reachable by the PPS, TS, CS, RPS, PRS, right RRS, and RRS serial chains. It is interesting how quickly the complexity of the problem increases with the number of dimensional parameters and the degree of the surface. The total degree of the polynomial systems that we consider range from 32 for the simplest to over 4 million for the most complex.

We show that these polynomial systems have a generalized linear product structure [9] that yields a bound on the number of solutions that ranges from 10 to over 800,000. In addition, this generalized linear product structure provides a convenient start system for a homotopy algorithm POLSYS\_GLP developed for this application to numerically determine all of the solutions of these polynomial systems [10,11].

Our results are summarized in Table 3 which compares the total degree of each polynomial system, the bound obtained using the generalized linear product structure of these polynomials, and the number of solutions obtained using the homotopy algorithm POLSYS\_GLP.

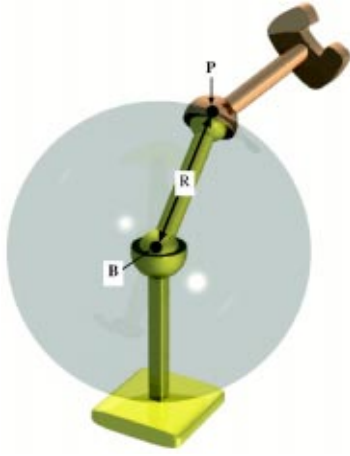
## 2 Homotopy Algorithms

Our concern is finding all of the solutions of a set of  $n$  polynomial equations in  $n$  unknowns that arise in finding surfaces reachable by articulated chains. For the cases of the plane and sphere, the systems of polynomials can be solved by direct elimination of the unknown parameters to obtain a univariate polynomial. Numerical solution of this polynomial, combined with back-substitution yields the desired solutions. However, the remaining surfaces yield systems of polynomials that are simply too complicated to solve by direct parameter elimination, therefore we use a numerical method called a homotopy algorithm.

Consider the array of polynomials Eq. (2) obtained from Eq. (1),

$$P(\mathbf{z}) = \begin{Bmatrix} S_1(\mathbf{z}) \\ S_2(\mathbf{z}) \\ \vdots \\ S_7(\mathbf{z}) \end{Bmatrix} = 0, \quad (2)$$

where  $\mathbf{z} = (\mathbf{p}, \mathbf{B}, R)$  is the vector of parameters that define the sphere. If we start with a polynomial system  $Q(\mathbf{z}) = 0$  that has the



**Fig. 1** A sphere traced by a point at the wrist center of a TS serial chain

same structure as  $P(\mathbf{z})=0$  but with a known set of solutions, then we can continuously transform  $Q(\mathbf{z})$  into  $P(\mathbf{z})$  and track its roots in order to find the solutions of  $P(\mathbf{z})=0$ . This continuous transformation of  $Q(\mathbf{z})$  into  $P(\mathbf{z})$  is called a *homotopy* map.

A numerical homotopy technique was used by Tsai and Morgan [12] to solve the inverse kinematics equations of a general 6R robot manipulator. Wampler et al. [13] and Sommese et al. [14] describe the use of numerical homotopy for applications in the kinematics of linkages and robots. Our focus on the design of serial chain robots follows [15], who used numerical homotopy to solve the design equations for an RRR manipulator.

For our purposes, we use the convex combination homotopy map Eq. (3)

$$H(\lambda, \mathbf{z}) = (1 - \lambda)Q(\mathbf{z}) + \lambda P(\mathbf{z}), \quad (3)$$

where  $\lambda \in [0, 1)$  is the real-valued homotopy parameter. The coefficients of our polynomial system  $P(\mathbf{z})=0$  are real, however, its roots  $\mathbf{z}$  need not be. Therefore, the homotopy  $H(\lambda, \mathbf{z})$  must be viewed as an array of  $n$  complex functions in  $n$  complex variables  $\mathbf{z}$  together with a single real variable  $\lambda$ .

For each root of the start system  $Q(\mathbf{z})=0$ , denoted  $\mathbf{z}=\mathbf{a}_j$ ,  $j=1, \dots, N$ , the homotopy equation  $H(\lambda, \mathbf{z})=0$  has an associated zero curve  $\gamma_a$ , which is the connected component of  $H^{-1}(0)$  containing the start point  $(0, \mathbf{a}_j)$ . The zero curve leads either to a point  $(1, \mathbf{z}_a)$  where  $P(\mathbf{z}_a)=0$ , or diverges to a root “at infinity.”

Each zero curve can be parameterized by its arc length  $s$ , so  $\gamma_a$  has the form  $(\lambda(s), \mathbf{z}(s))$ . Tracking this curve involves numerical computation of points  $\mathbf{y}_i \approx (\lambda(s_i), \mathbf{z}(s_i))$ , where  $\{s_i\}$  is an increasing sequence of arc lengths. This can be done using a predictor-corrector strategy described in [11, 16].

Along the zero curve  $\gamma_a$ , we have  $H(\lambda(s), \mathbf{z}(s))=0$ , therefore we can compute Eq. (4)

$$\frac{d}{ds}H(\lambda, \mathbf{z}) = \begin{bmatrix} H_\lambda & H_z \end{bmatrix} \begin{bmatrix} d\lambda/ds \\ d\mathbf{z}/ds \end{bmatrix} = 0, \quad (4)$$

where  $[J_H] = [H_\lambda, H_z]$  is the  $n \times (n+1)$  matrix of partial derivatives of the homotopy  $H(\lambda, \mathbf{z})$ . Notice that the vector  $\mathbf{v} = (d\lambda/ds, d\mathbf{z}/ds)^T$  tangent to the zero curve  $\gamma_a$  is in the nullspace of the Jacobian matrix  $[J_H]$ . This null space has dimension one by the theory of polynomial homotopy maps [11, 13].

The unit tangent vector  $\mathbf{v}_i$ , in the direction of increasing arc length, at a point  $\mathbf{y}_i$  on  $\gamma_a$  is used to predict a value for the next point  $\mathbf{y}_{i+1}^0$ , that is Eq. (5)

$$\mathbf{y}_{i+1}^0 = \mathbf{y}_i + (s_{i+1} - s_i)\mathbf{v}_i, \quad (5)$$

where  $s_{i+1} - s_i$  is a chosen arc length step. The predicted value of  $\mathbf{y}_{i+1}^0$  is corrected using the Taylor series expansion of the homotopy given by Eq. (6)

$$H(\mathbf{y}_{i+1}^0) + [J_H(\mathbf{y}_{i+1}^0)](\mathbf{y}_{i+1}^1 - \mathbf{y}_{i+1}^0) \approx 0, \quad (6)$$

which yields the correction formula Eq. (7)

$$\mathbf{y}_{i+1}^1 = \mathbf{y}_{i+1}^0 - [J_H(\mathbf{y}_{i+1}^0)]^\dagger H(\mathbf{y}_{i+1}^0). \quad (7)$$

The dagger denotes the Moore-Penrose pseudoinverse of the  $n \times (n+1)$  Jacobian matrix. Geometrically, iteration of the correction formula moves  $\mathbf{y}_{i+1}^k$  toward the zero curve  $\gamma_a$  along a normal direction, and is termed the “normal flow algorithm.”

The predictor can be improved by interpolation at previous computed points along the zero curve, and a projective transformation can be used to bound the arc length of all of the paths so that none diverge to infinity. Finally, an “end-game” strategy can improve the calculation of  $\mathbf{y}$  near  $\lambda=1$ . See [11] for details.

Fundamental to this approach to solving the equations  $P(\mathbf{z})=0$  is the determination of a start system  $Q(\mathbf{z})=0$  with a known set of solutions. A general purpose homotopy algorithm must systematically construct a start system with known roots that is appropriate for the given set of polynomials. In the next section, we show how to construct a start system using a generalized linear product representation of the system of polynomials.

### 3 Linear Product Decomposition

The fundamental theorem of algebra states that the number of roots of a polynomial is equal to or less than its degree, which is the integer value of its highest power—equality is obtained if roots are counted with the appropriate multiplicity. This has been generalized to Bezout’s theorem which states that the number of roots of a system of polynomials is less than or equal to the product of the degrees of the individual polynomials, called the *total degree* of the system. This fact leads to a relatively simple start system  $Q(\mathbf{z})=0$ , where  $d_i$ ,  $i=1, \dots, n$  is the degree of the  $i$ th polynomial in the target system  $P(\mathbf{z})=0$ , given by Eq. (8)

$$Q(\mathbf{z}) = \begin{cases} a_1 z_1^{d_1} - b_1 \\ a_2 z_2^{d_2} - b_2 \\ \vdots \\ a_n z_n^{d_n} - b_n \end{cases} = 0. \quad (8)$$

The coefficients  $a_i$  and  $b_i$  are randomly selected complex numbers. The solutions to this start system are easy to determine and provide the starting coordinates for tracing the  $d=d_1 d_2 \dots d_n$  zero curves to the solutions of  $P(\mathbf{z})=0$ .

In the problems that we consider in this paper, the total degree over-estimates the number of roots in the target polynomial  $P(\mathbf{z})$  by a significant amount. For example in order to solve our example problem Eq. (1) the polynomial homotopy algorithm with the start system Eq. (8) would track 128 paths to find 20 roots, which means over 80% of the computation is spent tracing paths that are extraneous.

The problem of extraneous paths arises from the fact that the polynomials we wish to solve are not general, but instead have internal structure that reduces the number of solutions. Morgan et al. [9] show that a “generic” system of polynomials that includes every monomial of a particular system of polynomials will have as many or more solutions as any version obtained by specifying values for the coefficients. This leads to the construction of the *linear product decomposition* of a system of polynomials. Associated with a linear product decomposition is a start system that is easy to construct and solve called the *generalized linear product*.

In order to illustrate the linear product decomposition, we analyze the example Eq. (1) in more details. Write these polynomials in vector form to obtain Eq. (9)

$$(\mathbf{P}^i - \mathbf{B}) \cdot (\mathbf{P}^i - \mathbf{B}) = R^2, \quad i=1, \dots, 7, \quad (9)$$

where the dot denotes the vector dot product. Now subtract the first equation from the rest in order to eliminate  $R^2$ . This reduces the problem to six equations in the unknowns  $\mathbf{z} = (x, y, z, u, v, w)$ , given by Eq. (10)

$$S(\mathbf{z}) = \begin{Bmatrix} (\mathbf{P}^2 \cdot \mathbf{P}^2 - \mathbf{P}^1 \cdot \mathbf{P}^1) - 2\mathbf{B} \cdot (\mathbf{P}^2 - \mathbf{P}^1) \\ \vdots \\ (\mathbf{P}^7 \cdot \mathbf{P}^7 - \mathbf{P}^1 \cdot \mathbf{P}^1) - 2\mathbf{B} \cdot (\mathbf{P}^7 - \mathbf{P}^1) \end{Bmatrix} = 0. \quad (10)$$

Realizing the fact that  $\mathbf{P}^j \cdot \mathbf{P}^j - \mathbf{P}^1 \cdot \mathbf{P}^1$  ( $j=2, \dots, 7$ ) is linear in terms of  $x, y$  and  $z$ , it is not hard to verify that a generic set of polynomials that contains our system as a special case can be constructed as a product of linear factors, as

$$Q(\mathbf{z}) = \begin{Bmatrix} (a_1x + b_1y + c_1z + d_1)(e_1u + f_1v + g_1w + h_1) \\ \vdots \\ (a_6x + b_6y + c_6z + d_6)(e_6u + f_6v + g_6w + h_6) \end{Bmatrix} = 0, \quad (11)$$

where the coefficients are known complex constants. This structure is called the *linear product decomposition* of the target system.

Solutions to a linear product decomposition of a set of polynomials are easily determined by assembling all combinations of factors, one from each equation, that can be set to zero and solved for the unknown parameters [17]. In our example, select three factors  $a_ix + b_iy + c_iz + d_i = 0$  from the six equations, and combine with the three factors  $e_iv + f_iv + g_iw + h_i = 0$  in the remaining equations. A solution of this set of six linear equations is a root of Eq. (11). Thus, we find that this system has  $\binom{6}{3} = 20$  solutions, which matches the known result for Eq. (10).

For the problems we consider the linear product decomposition provides a bound on the number of solutions that is significantly less than the total degree.

#### 4 Generalized Linear Product

The ‘‘generalized linear product’’ is a start system constructed from the linear product decomposition of a polynomial system. It is an extended version of the ‘‘partitioned linear product’’ used to construct  $m$ -homogeneous start systems [11].

We begin with a linear product decomposition for each of the polynomials  $P_i$ ,  $i=1, \dots, n$  in the unknowns  $z_i$ ,  $i=1, \dots, n$ . Augment each factor in this decomposition with a constant term, if it is not already present. This means that a factor of the form  $\langle z_1, z_2, z_3 \rangle$  is replaced by  $\langle z_1, z_2, z_3, 1 \rangle$ . Now for notational convenience we introduce the ‘‘mask’’  $S_{ij} = (s_{ij1}, \dots, s_{ijn})$  constructed from  $n$  1s and 0s in order to identify the unknowns in  $\mathbf{z} = (z_1, z_2, \dots, z_n)$  that appear in a specific linear factor. This allows us to write a general linear product decomposition as Eq. (12)

$$P_i \in \prod_{j=1}^{m_i} \langle s_{ij1}z_1, \dots, s_{ijn}z_n, 1 \rangle^{d_{ij}}, \quad (12)$$

where  $m_i$  is the number of different factors in polynomial  $P_i$ . Notice that  $d_i = \sum_{j=1}^{m_i} d_{ij}$  is the degree of  $P_i$ . This decomposition is specified by identifying the masks  $S_{ij}$  and the associated degrees  $d_{ij}$ .

We now construct the start system by introducing the polynomial Eq. (13)

$$G_{ij} = \left( \sum_{k=1}^n c_{ijk} s_{ijk} z_k \right)^{d_{ij}} - 1, \quad (13)$$

for each factor in the augmented linear product decomposition. The coefficients  $c_{ijk}$  are randomly specified complex numbers. Thus, the generalized linear product start system is given by Eq. (14)

$$Q(\mathbf{z}) = \begin{Bmatrix} \prod_{j=1}^{m_1} G_{1j} \\ \vdots \\ \prod_{j=1}^{m_n} G_{nj} \end{Bmatrix}. \quad (14)$$

In order to determine the roots of this start system, we follow [11] and introduce the *factor lexicographic vector*  $\Phi = (\Phi_1, \Phi_2, \dots, \Phi_n)$  which is the lexicographically ordered combinations of factors taken one from each polynomial in the system. Notice that  $\Phi$  ranges from  $(1, 1, \dots, 1) \leq \Phi \leq (m_1, m_2, \dots, m_n)$ . Next, we introduce the *degree lexicographic vector*  $\Delta = (\Delta_1, \Delta_2, \dots, \Delta_n)$  which is the lexicographically ordered combinations of the count of the roots of unity associated with the degree of the factor. The set  $\Delta$  ranges from  $(0, 0, \dots, 0) \leq \Delta \leq (d_{1\Phi_1} - 1, d_{2\Phi_2} - 1, \dots, d_{n\Phi_n} - 1)$ , where  $1 \leq d_{i\Phi_i}$  by definition of our linear product decomposition.

Given a combination of factors  $\Phi$ , we have one or more arrays  $\Delta$  depending on the degrees of the specific factors identified by  $\Phi$ . These two vectors specify the linear system of equations Eq. (15)

$$[A_\Phi] \mathbf{z} = \begin{Bmatrix} \sum_{k=1}^{m_1} c_{1\Phi_1 k} s_{1\Phi_1 k} z_k \\ \sum_{k=1}^{m_2} c_{2\Phi_2 k} s_{2\Phi_2 k} z_k \\ \vdots \\ \sum_{k=1}^{m_n} c_{n\Phi_n k} s_{n\Phi_n k} z_k \end{Bmatrix} = \begin{Bmatrix} e^{i\Delta_1/d_{1\Phi_1}} \\ e^{i\Delta_2/d_{2\Phi_2}} \\ \vdots \\ e^{i\Delta_n/d_{n\Phi_n}} \end{Bmatrix} = b_\Delta. \quad (15)$$

If  $[A_\Phi]$  is non-singular then the solution of this equation contributes a root to the start system for every root of unity in the array  $\Delta$ . Wise et al. [11] provide an efficient algorithm for computing the solutions to linear systems that are organized in this way, which was implemented in the polynomial homotopy software POLSYS\_PLP. We use the same algorithm to determine the roots of our generalized linear product start systems. For this reason, we term our algorithm POLSYS\_GLP.

#### 5 Verifying the Linear Product Decomposition

In order to execute POLSYS\_GLP, the user provides both the target polynomials and their associated linear product decompositions, which are used to construct the start system. If there is an error and the polynomial does not actually lie in the span of the specified generic linear products, then the homotopy is meaningless. Therefore, it is imperative to verify the linear product decomposition as follows.

For each polynomial  $P_i$ , we check that each monomial  $z_1^{\alpha_1} z_2^{\alpha_2} \dots z_n^{\alpha_n}$  is contained in the associated linear product decomposition  $\prod_{j=1}^{m_i} \langle s_{ij1}z_1, \dots, s_{ijn}z_n, 1 \rangle^{d_{ij}}$ . Our approach is to create a ‘‘set structure table’’ that has the linear terms of  $\langle s_{ij1}z_1, \dots, s_{ijn}z_n, 1 \rangle$  as its column headings, and the factors of the expanded monomial  $z_1^{\alpha_1} z_2^{\alpha_2} \dots z_n^{\alpha_n}$  as its rows. This set structure table has as many columns as the total degree  $d_i$  of  $P_i$ , and as many rows as the total degree of the monomial, which must be less than or equal to  $d_i$ .

The defining characteristic of a linear product decomposition is that each factor of the expanded monomial arises from a different linear term in the decomposition. This means that each row of the set structure table must be assignable to a separate column. If this assignment does not exist then the linear decomposition is invalid.

We begin with the first row and search the columns left to right to find a linear term (column) that contains the associated monomial factor (row). This column number is saved in a list that

denotes the linear terms that have been taken. The row is incremented and the search applied to the columns that have not been taken. When the final row is assigned to an available linear term the verification for the monomial is complete.

If a row is found to have a factor that cannot be assigned to a linear term, then the assignment of the factor in the previous row is advanced to the next linear term (column) in which it is contained. This step continues until either all of the factors are assigned to separate columns, or there is no available assignment for the factor in the first row. If this occurs then the monomial is not contained in the span of the linear product decomposition.

## 6 Parallelizing the Path Tracking Step

Each solution of the GLP start system Eq. (15) defines a starting point to begin tracing an individual zero curve. The zero curve for every root must be traced to determine whether it leads to a root of the target system or to a point at infinity. Because these calculations are independent, they can be distributed among different processors in a parallel computing cluster. See [18–21].

We use MPI-2 (Message Passing Interface) described by Gropp et al. [22] to distribute an identical set of POLSYS\_GLP routines among each of  $n-1$  slave processing nodes, numbered  $r = 1, \dots, n-1$ . The number  $r$  is called the *rank* of the processor. The processor of rank 0 is the master node. Each of the slave nodes executes a loop consisting of a request to the master node for a path index. This index identifies the root that begins a particular zero curve. The slave node traces the zero curve, reports the results and requests another path index. The master node receives the requests by the slave nodes, identifies the rank of the requesting node, distributes the next path index, and sends a stop code when all the paths are traced.

Recall that the start system is constructed using random values for the coefficients in the polynomials  $G_{ij}$ . We generate these coefficients separately and provided them to the slave routines via a data file. In this way each slave node has the same start system with the same array of roots. This reduces the need for inter-processor communication. The result is a convenient parallel computation of the homotopy zero curves leading from the roots of the start system to the roots of the target polynomial system.

## 7 Computation of Reachable Surfaces




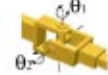

We now consider the problem of finding surfaces that contain a set of points generated by a displaced rigid body. Our focus is on the surfaces reachable by the wrist center of an articulated serial chain. In general, each joint of an articulated serial chain is designed to allow either pure rotation about, or a linear slide along, the joint axis, and is termed a revolute or prismatic joint, denoted R and P, respectively. See [23] for an introduction to the kinematics of articulated serial chains.

Revolute and prismatic joints can be combined to define other specialized joints. In particular, the sequence of two revolute joints that have axes that intersect at right angles is called a gimbal, or universal joint, denoted by a T. Similarly, the sequence of a revolute and a prismatic joint constructed so their axes are parallel is called a cylindrical (C) joint. Finally, a three revolute chain with concurrent joint axes form a spherical (S), or ball, joint. See Table 1.

A spherical wrist is an S-joint that allows full orientation of the gripper about its wrist center,  $\mathbf{P}$ , therefore our reachable surfaces by  $\mathbf{P}$  under the control of two other joints in the articulated chain. The combinations available for revolute and prismatic joints yields four basic chains: PPS, RPS, PRS, and RRS. The reachable surfaces defined by these chains are the plane, the circular hyperboloid, the elliptic cylinder and the general torus.

We can obtain additional reachable surfaces by specializing the dimensional parameters that characterize the first two joints. In particular, the RR chain has two defining parameters the distance,  $\rho$ , between the joint axes along their common normal line, and the angle  $\alpha$  between them measured around this common normal. For

Table 1 The five basic joints

Joint	Diagram	Symbol	DOF
Revolute		R	1
Prismatic		P	1
Cylindric		C	2
Universal		T	2
Spherical		S	3

$\alpha = \pi/2$  we have the chain “right” RRS that traces a circular torus. For the case  $\alpha=0$ , the “parallel” RRS traces a plane and is equivalent to the PPS chain. If the parameter  $\rho=0$ , then the surface is part of a sphere, and fills the sphere for  $\alpha = \pi/2$  which characterizes a TS chain.

For RP and PR chains, only the angle  $\alpha$  is important because this joint ensures that all points to travel on lines parallel to its direction. We can identify the special cases of the RPS and PRS for which this angle is  $\alpha=0$ , which in both cases become the CS chain that traces a circular cylinder. If this angle is  $\alpha = \pi/2$ , called a “right” RPS, then the surface is again a plane equivalent to that traced by the PPS chain.

Finally, all PP chains are essentially the same as long as the directions of the two joints are not parallel, so that some component of movement perpendicular to the first prismatic joint is available by sliding along the second joint.

The result is a set of seven algebraic surfaces that are reachable by the wrist centers of a set of articulated chains. See Table 2.

In what follows, we let matrices  $[T_i] = [A_i, \mathbf{d}_i]$ ,  $i = 1, \dots, n$  denote the  $n$  given spatial displacements which the end-effector must reach,  $[A_i]$  is a  $3 \times 3$  rotation matrix and  $\mathbf{d}_i$  is a  $3 \times 1$  translation vector. And we consider a point  $\mathbf{p} = (x, y, z)^T$  in a moving body. The images of this point on the spatial displacements define the set of points  $\mathbf{P}^i = (X_i, Y_i, Z_i)^T = [A_i]\mathbf{p} + \mathbf{d}_i$ . The sets of polynomial equations are formulated by requiring these image points  $\mathbf{P}^i$  lie on the seven reachable surfaces. We then provide a linear product decomposition and the results of our polynomial homotopy solution. Once the reachable surfaces are determined, we can compute the dimensions of corresponding serial chains.

**7.1 The Plane.** The PPS serial chain has the property that the wrist center  $\mathbf{P}^i = (X, Y, Z)$  is constrained to lie on a plane with normal  $\mathbf{G} = (a, b, c)$  (Fig. 2), that is

$$\mathbf{G} \cdot \mathbf{P}^i - d = 0, \quad i = 1, \dots, 6. \quad (16)$$

Table 2 The basic serial chains and their associated reachable surfaces

Case	Chain	angle	length	Surface
1	PPS	–	–	plane
2	TS	$\pi/2$	0	sphere
3	CS	0	–	circular cylinder
4	RPS	$\alpha$	–	circular hyperboloid
5	PRS	$\alpha$	–	elliptic cylinder
6	right RRS	$\pi/2$	$\rho$	circular torus
7	RRS	$\alpha$	$\rho$	general torus

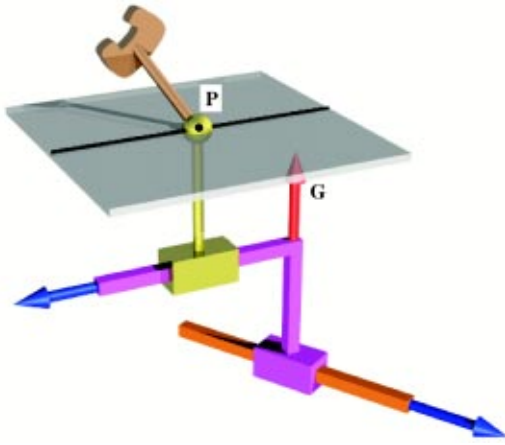


Fig. 2 A plane as traced by a point at the wrist center of a PPS serial chain

The parameter  $d$  is the product of the magnitude  $|G|$  and the signed normal distance to the plane. We set  $n=6$  because there are only six independent unknowns in Eq. (16), two coordinates of  $G$ , the three coordinates of  $p$ , and  $d$ . Notice, the components of  $G$  are not independent because only the direction of  $G$  matters, not its magnitude. A convenient way to constrain this magnitude is to choose a vector  $m$  and scalar  $e$ , and require that  $G \cdot m = e$ .

Subtract the first of Eq. (16) from the remaining to eliminate  $d$  and assemble the constraint equation, we obtain the polynomial system

$$P(z) = \begin{cases} G \cdot (P^2 - P^1) \\ \vdots \\ G \cdot (P^6 - P^1) \\ G \cdot m - e \end{cases} = 0. \quad (17)$$

This is a set of five quadratic equations and one linear equation in the six unknowns  $z = (a, b, c, x, y, z)$ . The total degree of this system is  $2^5 = 32$ .

It is easy to see that this polynomial system has a bilinear structure with the LPD bound  $\binom{5}{2} = 10$ , which means that may be as many as 10 points in the moving body that lie on a plane for six specified positions of the end-effector. This system of polynomials Eq. (17) is small enough that direct elimination of the parameters can be used to obtain a univariate polynomial, which is found to be of degree 10.

Once the plane  $P$  and point  $p$  are defined, then it is possible to determine a PPS chain, a parallel RRS or a right RPS chain that guides this point through the specified positions.

**7.2 The Sphere.** We now return to our opening example in which  $n$  points  $P^i = (X_i, Y_i, Z_i)$  constrained to lie on a sphere of radius  $R$  around the point  $B = (u, v, w)$ , Fig. 1. This problem has seven parameters, the three components each of  $p$  and  $B$  and the radius  $R$ . Therefore we can evaluate Eq. (1) on  $n=7$  displacements,

$$(P^i - B)^2 - R^2 = 0, \quad i = 1, \dots, 7. \quad (18)$$

Subtract the first equation from the remainder in order to eliminate  $R$ , and obtain Eq. (10) where  $z = (x, y, z, u, v, w)$ .

System Eq. (18) has the linear product decomposition as shown in Eq. (11), from which we can compute the LPD bound  $\binom{6}{2} = 20$ . Parameter elimination yields a univariate polynomial of degree 20, which means that this bound is exact. Innocenti [24] presents an example that results in 20 real roots.

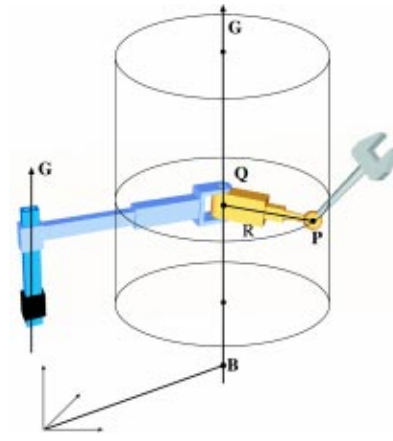


Fig. 3 The circular cylinder reachable by a CS serial chain

Thus, given seven arbitrary spatial positions there can be as many as 20 points in the moving body that have positions lying on a sphere. For each real point, it is possible to determine an associated TS chain.

**7.3 The Circular Cylinder.** In order to define the equation of a circular cylinder, let the line  $L(t) = B + tG$  be its axis. A general point  $P$  on the cylinder lies on a circle about the point  $Q$  closest to it on the axis  $L(t)$ . See Fig. 3.

By the geometry, the image points  $P^i$  of the spherical wrist must satisfy the circular cylinder equation

$$((P^i - B) \times G)^2 - R^2 G^2 = 0, \quad i = 1, \dots, 8. \quad (19)$$

See [25] for the details on deriving the cylinder equation.

We set  $n=8$  because Eq. (19) have only eight independent parameters, the radius  $R$ , three for  $P = (X, Y, Z)$ , two for  $B = (u, v, w)$  and two for  $G = (a, b, c)$ . Notice only the direction of  $G$  matters not its magnitude, we choose an arbitrary vector  $m$  and scalar  $e$  and require the components of  $G$  satisfy the constraint  $G \cdot m - e = 0$ . The components of the point  $B$  are also not independent, but for a different reason. It is because any point on the line  $L(t)$  can be selected as the reference point  $B$ . We identify this point by requiring  $B$  to lie on a specific plane  $U: (n, f)$ , that is  $B \cdot n - f = 0$ , where  $n$  and  $f$  are chosen arbitrarily to avoid the possibility that the line  $L(t)$  may lie entirely on  $U$ .

Subtract the first of Eq. (19) from the remaining seven to eliminate  $R$  and assemble with two constraint equations to define the system of polynomials

$$C(z) = \begin{cases} (P^2 \times G)^2 - (P^1 \times G)^2 - 2((P^2 - P^1) \times G) \cdot (B \times G) \\ \vdots \\ (P^8 \times G)^2 - (P^1 \times G)^2 - 2((P^8 - P^1) \times G) \cdot (B \times G) \\ G \cdot m - e \\ B \cdot n - f \end{cases} = 0. \quad (20)$$

Notice we have expanded the dot products in Eq. (19). This is a set of seven polynomials of degree four and two of degree one. The total degree is  $4^7 = 16,384$ . See [25,26] for additional details about this problem.

A linear product decomposition for the polynomial system Eq. (20) is provided in [25]. The LPD bound is 2184 which is significantly less than the total degree. We use our POLSYS\_GLP homotopy algorithm to determine the roots for this system of polynomials for a random set of test cases and obtain the exact root count for this problem as 804. Thus, for eight arbitrary spatial positions we can find as many as 804 points in the moving body each of which has all eight positions on a circular cylinder. For each of these points, we can determine an associated CS chain.

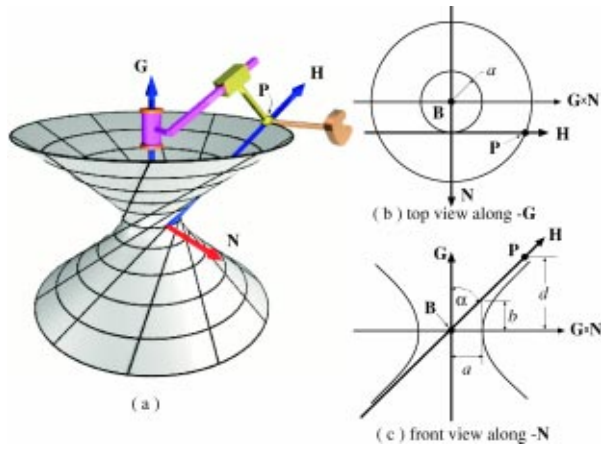


Fig. 4 The circular hyperboloid traced by the wrist center of an RPS serial chain

**7.4 The Circular Hyperboloid.** A circular hyperboloid is generated by rotating one line around another so that every point on the moving line traces a circle around the fixed line,  $\mathbf{G}$ , which is the axis of the hyperboloid, Fig. 4. Of all of these circles there

is one with the smallest radius,  $R$ , and its center  $\mathbf{B}=(u,v,w)$  is the center of the hyperboloid.

By the geometry, a point  $\mathbf{P}$  on the circular hyperboloid must satisfy the following equation

$$(\mathbf{P}-\mathbf{B})^2 - ((\mathbf{P}-\mathbf{B}) \cdot \mathbf{G})^2 \left( \frac{1 + \tan^2 \alpha}{\mathbf{G} \cdot \mathbf{G}} \right) - R^2 = 0. \quad (21)$$

See [27] for details deriving the hyperboloid equation.

Expand Eq. (21) and collect terms to obtain

$$k_0 \mathbf{P} \cdot \mathbf{P} + 2 \mathbf{K} \cdot \mathbf{P} - (\mathbf{P} \cdot \mathbf{G})^2 - \zeta = 0, \quad (22)$$

where we have introduced the parameters  $k_0$ ,  $\mathbf{K}=(k_1, k_2, k_3)$  and  $\zeta$  defined by

$$k_0 = \frac{\mathbf{G} \cdot \mathbf{G}}{1 + \tan^2 \alpha}, \quad \mathbf{K} = (\mathbf{B} \cdot \mathbf{G}) \mathbf{G} - k_0 \mathbf{B}, \quad \zeta = (\mathbf{B} \cdot \mathbf{G})^2 - k_0 \mathbf{B} \cdot \mathbf{B} + k_0 R^2.$$

Thus, the 11 dimensional parameters  $\zeta$ ,  $k_0$ ,  $\mathbf{K}$ ,  $\mathbf{G}$ , and  $\mathbf{P}$  define a circular hyperboloid.

As we have seen previously, it is the direction of  $\mathbf{G}$  and not its magnitude that is required, so this magnitude can be set using an arbitrary vector  $\mathbf{m}$  and scalar  $e$  in the constraint equation  $\mathbf{G} \cdot \mathbf{m} - e = 0$ .

Evaluating Eq. (22) with the image points  $\mathbf{P}^i (i=1, \dots, 10)$  yields 10 polynomial equations. Subtract the first of these equations from the remaining in order to eliminate  $\zeta$  and assemble with the constraint equation  $\mathbf{G} \cdot \mathbf{m} - e = 0$ , we can obtain the system of polynomial equations

$$H(\mathbf{z}) = \begin{cases} k_0(\mathbf{P}^2 \cdot \mathbf{P}^2 - \mathbf{P}^1 \cdot \mathbf{P}^1) + 2\mathbf{K} \cdot (\mathbf{P}^2 - \mathbf{P}^1) - (\mathbf{P}^2 \cdot \mathbf{G})^2 + (\mathbf{P}^1 \cdot \mathbf{G})^2 \\ \vdots \\ k_0(\mathbf{P}^{10} \cdot \mathbf{P}^{10} - \mathbf{P}^1 \cdot \mathbf{P}^1) + 2\mathbf{K} \cdot (\mathbf{P}^{10} - \mathbf{P}^1) - (\mathbf{P}^{10} \cdot \mathbf{G})^2 + (\mathbf{P}^1 \cdot \mathbf{G})^2 \\ \mathbf{G} \cdot \mathbf{m} - e \end{cases} = 0. \quad (23)$$

Equation (23) is a system of nine fourth degree polynomials and one linear equation which has a total degree of  $4^9 = 262,144$ . See [26,28] for other formulations of this problem.

A linear product decomposition for this polynomial system is provided in [27]. The LPD bound is 9216. Our POLSYS\_GLP algorithm yielded a generic root count of 1024 among the 9216 homotopy paths. This calculation took approximately 24 hours on a single 2.4GHz PC (384 paths/processor-hour). The parallel version of POLSYS\_GLP was run on 8 64-bit processors of UCI's Beowulf cluster, and required 30 minutes (2304 paths/processor-hour). This particular problem has a structure that is convenient for polyhedral homotopy algorithms, which yield the same solutions in minutes on a single processor by tracking only 1024 paths [29].

Thus, for ten spatial positions, we can find as many as 1024 points that have all 10 positions on a circular hyperboloid. For each of these points we can find an associated RPS chain.

**7.5 The Elliptic Cylinder.** An elliptic cylinder is generated by a circle that has its center swept along a line  $L(t) = \mathbf{B} + t\mathbf{S}_1$  such that the vector through the center normal to the plane of the circle maintains a constant direction  $\mathbf{S}_2$  at an angle  $\alpha$  relative to the direction  $\mathbf{S}_1$  of  $L(t)$ , see Fig. 5. The major axis of the elliptic cross-section is the radius  $R$  of the circle and the minor axis is  $R \cos \alpha$ . This surface is generated by the wrist center of a PRS chain that has its P-joint aligned with the axis  $L(t)$  and its R-joint positioned so its axis is along  $\mathbf{S}_2$ .

A point  $\mathbf{P}$  on the elliptic cylinder must satisfy

$$(\mathbf{S}_2 \times ((\mathbf{P} - \mathbf{B}) \times \mathbf{S}_1))^2 - R^2 (\mathbf{S}_1 \cdot \mathbf{S}_2)^2 = 0. \quad (24)$$

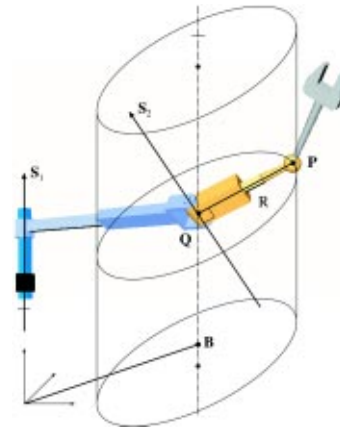


Fig. 5 The elliptic cylinder reachable by a PRS serial chain

See [25] for details on the derivation. To reduce the degree of Eq. (24), we expand the triple product and introduce new variables, that is Eq. (25)

$$\begin{aligned} \mathbf{S}_2 \times ((\mathbf{P} - \mathbf{B}) \times \mathbf{S}_1) &= (\mathbf{S}_1 \cdot \mathbf{S}_2)(\mathbf{P} - \mathbf{B}) - ((\mathbf{P} - \mathbf{B}) \cdot \mathbf{S}_2)\mathbf{S}_1 \\ &= (\mathbf{S}_1 \cdot \mathbf{S}_2)(\mathbf{P} - (\mathbf{P} \cdot \mathbf{K})\mathbf{S}_1 + \mathbf{Q}), \end{aligned} \quad (25)$$

where

$$\mathbf{K} = \frac{\mathbf{S}_2}{\mathbf{S}_1 \cdot \mathbf{S}_2}, \quad \text{and} \quad \mathbf{Q} = (\mathbf{B} \cdot \mathbf{K})\mathbf{S}_1 - \mathbf{B}.$$

We then add the constraints

$$\mathbf{S}_1 \cdot \mathbf{S}_1 = 1, \quad \mathbf{K} \cdot \mathbf{S}_1 = 1, \quad \text{and} \quad \mathbf{Q} \cdot \mathbf{K} = 0. \quad (26)$$

Notice that these definitions reduce the degree of the polynomials Eq. (24) from six to four after canceling  $(\mathbf{S}_1 \cdot \mathbf{S}_2)^2$ , that is

$$(\mathbf{P} - (\mathbf{P} \cdot \mathbf{K})\mathbf{S}_1 + \mathbf{Q})^2 - R^2 = 0. \quad (27)$$

Equation (27) have 13 unknowns the radius  $R$ , three for each of the vectors  $\mathbf{P}$ ,  $\mathbf{K}$ ,  $\mathbf{Q}$ ,  $\mathbf{S}_1$ . However only 10 of them are independent because of the constraints Eq. (26).

Evaluating Eq. (27) on the ten image points  $\mathbf{P}^i (i=1, \dots, 10)$  yields ten polynomial equation of degree four. We then subtract the first of these equations from the remaining and assemble the constraints Eq. (26) to obtain the polynomial system

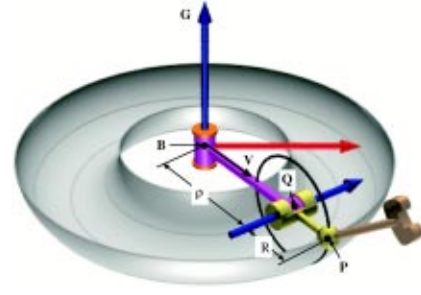
$$E(\mathbf{z}) = \left\{ \begin{array}{l} (\mathbf{P}^2 - (\mathbf{P}^2 \cdot \mathbf{K})\mathbf{S}_1 + \mathbf{Q})^2 - (\mathbf{P}^1 - (\mathbf{P}^1 \cdot \mathbf{K})\mathbf{S}_1 + \mathbf{Q})^2 \\ \vdots \\ (\mathbf{P}^{10} - (\mathbf{P}^{10} \cdot \mathbf{K})\mathbf{S}_1 + \mathbf{Q})^2 - (\mathbf{P}^1 - (\mathbf{P}^1 \cdot \mathbf{K})\mathbf{S}_1 + \mathbf{Q})^2 \\ \mathbf{S}_1 \cdot \mathbf{S}_1 - 1 \\ \mathbf{K} \cdot \mathbf{S}_1 - 1 \\ \mathbf{Q} \cdot \mathbf{K} \end{array} \right\} = 0, \quad (28)$$

which has the total degree  $4^9 2^3 = 2,097,152$ .

The best linear product decomposition of Eq. (28) we have found yields the LPD bound of 247,968, which is large. See details on the LPD structure in [30]. This system was solved using our parallelized POLSYS\_GLP on 128 nodes of the Blue Horizon supercomputer at the San Diego Supercomputer Center. The result was 18,120 solutions in almost 33 minutes. Because each node of Blue Horizon has eight processors, this corresponds to 563 cpu hours, or approximately 440 paths/processor-hour.

**7.6 The Circular Torus.** A circular torus is generated by sweeping a circle around an axis so its center traces a second circle. Let the axis be  $L(t) = \mathbf{B} + t\mathbf{G}$ , with Plucker coordinates  $\mathbf{G} = (\mathbf{G}, \mathbf{B} \times \mathbf{G})$ . See Fig. 6. Introduce a unit vector  $\mathbf{v}$  perpendicular to this axis so the center of the generating circle is given by  $\mathbf{Q} - \mathbf{B} = \rho\mathbf{v}$ . Now define  $\mathbf{u}$  to be the unit vector in the direction  $\mathbf{G}$ , then a point  $\mathbf{P}$  on the torus is defined by the vector equation,

$$\mathbf{P} - \mathbf{B} = \rho\mathbf{v} + R(\cos \phi\mathbf{v} + \sin \phi\mathbf{u}), \quad (29)$$



**Fig. 6 The circular torus traced by the wrist center of a "right" RRS serial chain**

where  $\phi$  is the angle measured from  $\mathbf{v}$  to the radius vector of the generating circle.

An algebraic equation of the torus is obtained from Eq. (29) by first computing the magnitude Eq. (30)

$$(\mathbf{P} - \mathbf{B})^2 = \rho^2 + R^2 + 2\rho R \cos \phi. \quad (30)$$

Next compute the dot product with  $\mathbf{u}$ , to obtain Eq. (31)

$$(\mathbf{P} - \mathbf{B}) \cdot \mathbf{u} = R \sin \phi. \quad (31)$$

Finally, eliminate  $\cos \phi$  and  $\sin \phi$  from these equations, and the result is

$$\mathbf{G}^2((\mathbf{P} - \mathbf{B})^2 - \rho^2 - R^2)^2 + 4\rho^2((\mathbf{P} - \mathbf{B}) \cdot \mathbf{G})^2 = 4\rho^2\mathbf{G}^2R^2. \quad (32)$$

This is the equation of a circular torus. It has 11 parameters, the scalars  $\rho$  and  $R$  and the three vectors  $\mathbf{G}$ ,  $\mathbf{P}$  and  $\mathbf{B}$ .

In order to simplify this system of polynomials we introduce the parameters

$$\mathbf{H} = 2\rho\mathbf{G} \quad \text{and} \quad k_1 = \mathbf{B}^2 - \rho^2 - R^2,$$

which yields the identity Eq. (33)

$$4\rho^2R^2 = \mathbf{H}^2 \left( \mathbf{B}^2 - \frac{\mathbf{H}^2}{4} - k_1 \right). \quad (33)$$

Substitute these relations into Eq. (32) which eliminates  $R^2$  and we obtain the system of 10 polynomials

$$T(\mathbf{z}) = \left\{ \begin{array}{l} ((\mathbf{P}^1)^2 - 2\mathbf{P}^1 \cdot \mathbf{B} + k_1)^2 + ((\mathbf{P}^1 - \mathbf{B}) \cdot \mathbf{H})^2 - \mathbf{H}^2 \left( \mathbf{B}^2 - \frac{\mathbf{H}^2}{4} - k_1 \right) \\ \vdots \\ ((\mathbf{P}^{10})^2 - 2\mathbf{P}^{10} \cdot \mathbf{B} + k_1)^2 + ((\mathbf{P}^{10} - \mathbf{B}) \cdot \mathbf{H})^2 - \mathbf{H}^2 \left( \mathbf{B}^2 - \frac{\mathbf{H}^2}{4} - k_1 \right) \end{array} \right\} = 0, \quad (34)$$

which has the total degree  $4^{10} = 1,048,576$ .

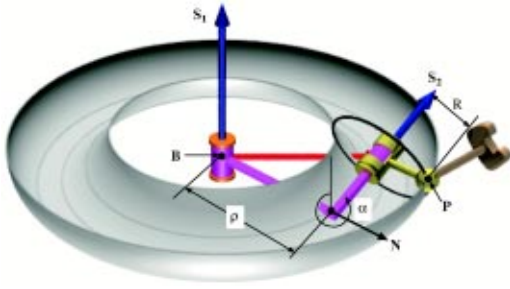
It is difficult to find a simplified formulation for these equations, even if we subtract the first equation from the remaining in order to cancel terms. The best linear product decomposition of Eq. (34) we have found yields the LPD bound of 868,352 which is not much different to the total degree. See [30] for the details on the LPD structure. The computation of these homotopy paths took 72 minutes on 128 nodes of the Blue Horizon supercomputer. This means the over 800,000 paths were tracked on 1024 processors at a rate of approximately 707 paths per hour.

**7.7 The General Torus.** A general torus is defined by sweeping a circle that has a general orientation in space around an arbitrary axis. See Fig. 7. Let  $\mathbf{S}_1 = (\mathbf{S}_1, \mathbf{B} \times \mathbf{S}_1)$  be the Plucker coordinates of the line that forms the axis of the torus, and  $\mathbf{S}_2$

$= (\mathbf{S}_2, \mathbf{Q} \times \mathbf{S}_2)$  be the through the center of the sweeping circle, perpendicular to its plane. These two lines define a common normal  $\mathbf{N}$  and we choose its intersection with  $\mathbf{S}_1$  and  $\mathbf{S}_2$  to be the reference points  $\mathbf{B}$  and  $\mathbf{Q}$ , respectively. The normal angle and distance between these lines around and along their common normal are denoted  $\alpha$  and  $\rho$ . Finally, we identify the center of the sweeping circle as lying a distance  $d$  along  $\mathbf{S}_2$  measured from  $\mathbf{Q}$ .

In this derivation, we constrain  $\mathbf{S}_1$  and  $\mathbf{S}_2$  to be unit vectors, in order to reduce the degree of the resulting equation. This allows us to define the unit vector in the common normal direction as  $\mathbf{n} = (\mathbf{S}_1 \times \mathbf{S}_2) / \sin \alpha$ , so we obtain a general point  $\mathbf{P}$  on the torus from the vector Eq. (35),

$$\mathbf{P} - \mathbf{B} = \rho\mathbf{n} + d\mathbf{S}_2 + R(\cos \phi\mathbf{n} + \sin \phi(\mathbf{S}_2 \times \mathbf{n})). \quad (35)$$



**Fig. 7** The general torus reachable by the wrist center of an RRS serial chain

The algebraic equation for the torus is obtained by first computing Eq. (36)

$$(\mathbf{P} - \mathbf{B})^2 = \rho^2 + d^2 + R^2 + 2\rho R \cos \phi, \quad (36)$$

and Eq. (37)

$$(\mathbf{P} - \mathbf{B}) \cdot (\mathbf{S}_2 \times \mathbf{n}) = R \sin \phi. \quad (37)$$

Notice that  $\mathbf{S}_2 \times \mathbf{n}$  is

$$\mathbf{S}_2 \times \frac{\mathbf{S}_1 \times \mathbf{S}_2}{\sin \alpha} = \frac{1}{\sin \alpha} (\mathbf{S}_1 - \cos \alpha \mathbf{S}_2).$$

Now, eliminate  $\phi$  between these two equations to obtain

$$\begin{aligned} & ((\mathbf{P} - \mathbf{B})^2 - \rho^2 - d^2 - R^2)^2 + \frac{4\rho^2}{\sin^2 \alpha} ((\mathbf{P} - \mathbf{B}) \cdot \mathbf{S}_1 - d \cos \alpha)^2 \\ & - 4\rho^2 R^2 = 0. \end{aligned} \quad (38)$$

This equation has four scalar parameters  $\rho$ ,  $\alpha$ ,  $d$  and  $R$ , and three vector parameters  $\mathbf{P}$ ,  $\mathbf{B}$  and  $\mathbf{S}_1$  which combine with the constraint,  $|\mathbf{S}_1| = 1$ , to yield 12 independent parameters.

**Table 3** Summary of the total degree, LPD bound, and number of solutions of the polynomial equations that define each reachable surface

Case	Surface	Total degree	LPD bound	Number of roots
1	plane	32	10	10
2	sphere	64	20	20
3	circular cylinder	16,384	2184	804
4	circular hyperboloid	262,144	9216	1024
5	elliptic cylinder	2,097,152	247,968	18,120
6	circular torus	2,097,152	868,352	94,622
7	general torus	4,194,304	448,702	42,615

In order to simplify the use of Eq. (38), we introduce the new parameters

$$k_1 = \mathbf{B} \cdot \mathbf{B} - \rho^2 - R^2 - d^2,$$

$$k_2 = (\mathbf{B} \cdot \mathbf{S}_1 + d \cos \alpha) \frac{2\rho}{\sin \alpha},$$

$$k_3 = 4\rho^2 R^2,$$

$$\mathbf{H} = \frac{2\rho}{\sin \alpha} \mathbf{S}_1,$$

This allow us to write Eq. (38) in the form

$$(\mathbf{P} \cdot \mathbf{P} - 2\mathbf{P} \cdot \mathbf{B} + k_1)^2 + (\mathbf{P} \cdot \mathbf{H} - k_2)^2 - k_3 = 0. \quad (39)$$

This is a quartic polynomial in the 12 unknowns, consisting of  $k_1, k_2, k_3$  and the components  $\mathbf{P}$ ,  $\mathbf{B}$  and  $\mathbf{H}$ .

We then evaluate Eq. (39) on the image points  $\mathbf{P}^i$  ( $i = 1, \dots, 12$ ) and obtain 12 polynomials of degree four. Subtract the first of these equations from the remaining to cancel  $k_3$  and obtain

$$G(\mathbf{z}) = \left\{ \begin{array}{l} (\mathbf{P}^2 \cdot \mathbf{P}^2 - 2\mathbf{P}^2 \cdot \mathbf{B} + k_1)^2 - (\mathbf{P}^1 \cdot \mathbf{P}^1 - 2\mathbf{P}^1 \cdot \mathbf{B} + k_1)^2 + (\mathbf{P}^2 \cdot \mathbf{H} - k_2)^2 - (\mathbf{P}^1 \cdot \mathbf{H} - k_2)^2 \\ \vdots \\ (\mathbf{P}^{12} \cdot \mathbf{P}^{12} - 2\mathbf{P}^{12} \cdot \mathbf{B} + k_1)^2 - (\mathbf{P}^1 \cdot \mathbf{P}^1 - 2\mathbf{P}^1 \cdot \mathbf{B} + k_1)^2 + (\mathbf{P}^{12} \cdot \mathbf{H} - k_2)^2 - (\mathbf{P}^1 \cdot \mathbf{H} - k_2)^2 \end{array} \right\} = 0. \quad (40)$$

The total degree of polynomials system Eq. (40) is  $4^{11} = 4,194,304$  with 11 unknowns  $k_1$ ,  $k_2$ ,  $\mathbf{P}$ ,  $\mathbf{B}$  and  $\mathbf{H}$ .

We can refine the estimate of the number of roots of this polynomial system by using the linear product decomposition. The best linear product decomposition we have found yields the LPD bound of 448,702 which is much lower than the total degree. See [30]. Our parallel POLSYS\_GLP algorithm computed 42,615 solutions in 42 minutes using 128 nodes of Blue Horizon. This is approximately 626 paths/processor-hour. Each real solution can be used to design an RRS chain to reach the specified displacements. The distribution and utility of these solutions requires further study.

## 8 Conclusion

In this paper, we seek points in a moving body that lie on seven algebraic surfaces that are reachable by an articulated chain with a spherical wrist, see Table 2. The algebraic equations of these *reachable surfaces* are evaluated for a specified set of spatial displacements, in order to define a system of polynomial equations that are solved to determine the surface.

The complexity of this problem increases with degree of the surface and the number of parameters that define it, and for all but the simplest cases we use a numerical homotopy algorithm to find all of the roots. Vector operations in the derivation of these equations yield a general linear product structure that allows us to show the number of roots is (often) less than the total degree of the system. This linear product bound defines the number of paths that we must track using our homotopy algorithm POLSYS\_GLP to find these roots. Table 3 summarizes the results of our analysis. Note that the task positions are chosen to be generic enough to allow the resulted polynomial systems have finite number of solutions.

Except for the plane and sphere, this is the first computation of the solutions for these polynomial systems. The three most challenging cases were the elliptic cylinder, right circular torus and the general torus, which correspond to the PRS, the right RRS, and general RRS chains. In these cases, our algorithm required the Blue Horizon supercomputer in order to compute tens of thousands of solutions. More research is required to increase the efficiency of the calculation and to evaluate the utility of each solution.

## Acknowledgements

The authors gratefully acknowledge the comments by the reviewers, the support of National Science Foundation award DMII 0218285, Air Force Office of Scientific Research Grant F49620-02-1-0090, and a grant of computation time provided through the UCI Academic Associates Program in conjunction with the San Diego Supercomputer Center.

## References

- [1] Burmester, L., 1886, *Lehrbuch der Kinematik*, Verlag Von Arthur Felix, Leipzig, Germany.
- [2] Suh, C. H., and Radcliffe, C. W., 1978, *Kinematics and Mechanism Design*, John Wiley and Sons, New York.
- [3] Sandor, G. N., and Erdman, A. G., 1984, *Advanced Mechanism Design: Analysis and Synthesis, Vol. 2*, Prentice-Hall, Englewood Cliffs, NJ.
- [4] McCarthy, J. M., 2000, *Geometric Design of Linkages*, Springer-Verlag, New York.
- [5] Chen, P., and Roth, B., 1967, "Design Equations for Finitely and Infinitesimally Separated Position Synthesis of Binary Link and Combined Link Chains," *ASME J. Eng. Ind.*, **91**, pp. 209–219.
- [6] Bottema, O., and Roth, B., 1979, *Theoretical Kinematics*, North Holland Press, NY.
- [7] McCarthy, J. M., 1990, *An Introduction to Theoretical Kinematics*, MIT Press, Cambridge, MA.
- [8] Liao, Q., and McCarthy, J. M., 2001, "On the Seven Position Synthesis of a 5-SS Platform Linkage," *ASME J. Mech. Des.*, **123**(1), pp. 74–79.
- [9] Morgan, A. P., Sommese, A. J., and Wampler, C. W., 1995, "A Product-Decomposition Bound for Bezout Numbers," *SIAM (Soc. Ind. Appl. Math.) J. Numer. Anal.*, **32**(4), pp. 1308–1325.
- [10] Verschelde, J., 1999, "Algorithm 795: PHCpack: A Generalpurpose Solver for Polynomial Systems by Homotopy Continuation," *ACM Trans. Math. Softw.*, **25**(2), pp. 251–276.
- [11] Wise, S. M., Sommese, A. J., and Watson, L. T., 2000, "Algorithm 801: POL\_SYS PLP: A Partitioned Linear Product Homotopy Code for Solving Polynomial Systems of Equations," *ACM Trans. Math. Softw.*, **26**(1), pp. 176–200.
- [12] Tsai, L.-W., and Morgan, A. P., 1985, "Solving the Kinematics of the Most General Six- and Five-Degree-of-Freedom Manipulators by Continuation Methods," *ASME J. Mech., Transm., Autom. Des.*, **107**, pp. 189–200.
- [13] Wampler, C. W., Morgan, A. P., and Sommese, A. J., 1990, "Numerical Continuation Methods for Solving Polynomial Systems Arising in Kinematics," *ASME J. Mech. Des.*, **112**(1), pp. 59–68.
- [14] Sommese, A. J., Verschelde, J., and Wampler, C. W., 2002, "Advances in Polynomial Continuation for Solving Problems in Kinematics," *Proc. 2002 ASME Design Engineering Technical Conferences*, paper no. DETC2002/MECH-34254, Sept. 29-Oct. 2, Montreal, Canada.
- [15] Lee, E., and Mavroidis, D., 2002, "Solving the Geometric Design Problem of Spatial 3R Robot Manipulators Using Polynomial Homotopy Continuation," *ASME J. Mech. Des.*, **124**(4), pp. 652–661.
- [16] Watson, L. T., Sosonkina, M., Melville, R. C., Morgan, A. P., and Walker, H. F., 1997, "Algorithm 777: HOMPCK90: A suite of Fortran 90 codes for globally convergent homotopy algorithms," *ACM Trans. Math. Softw.*, **23**(4), pp. 514–549.
- [17] Wampler, C., 1994, "An Efficient Start System for Multi-Homogeneous Polynomial Continuation," *Numer. Math.*, **66**, pp. 517–523.
- [18] Allison, D. C. S., Harimoto, S., and Watson, L. T., 1989, "The Granularity of Parallel Homotopy Algorithms for Polynomial Systems of Equations," *Int. J. Comput. Math.*, **29**, pp. 21–37.
- [19] Allison, D. C. S., Chakraborty, A., and Watson, L. T., 1989, "The Granularity of Parallel Homotopy Algorithms for Polynomial Systems of Equations," *J. Supercomputing*, **3**, pp. 5–20.
- [20] Chakraborty, A., Allison, D. C. S., Ribbens, C. J., and Watson, L. T., 1991, "Note on Unit Tangent Vector Computation for Homotopy Curve Tracking on a Hypercube," *Parallel Comput.*, **17**, pp. 1385–1395.
- [21] Chakraborty, A., Allison, D. C. S., Ribbens, C. J., and Watson, L. T., 1993, "The Parallel Complexity of Embedding Algorithms for the Solution of Systems of Nonlinear Equations," *IEEE Trans. Parallel Distrib. Systems*, **4**, pp. 458–465.
- [22] Gropp, W., Lusk, E., and Skjellum, A., *Using MPI, Portable Parallel Programming with the Message-Passing Interface*, second edition, The MIT Press, Cambridge, MA.
- [23] Craig, J. J., 1989, *Introduction to Robotics, Mechanics and Control*, Addison Wesley, Reading, MA.
- [24] Innocenti, C., 1995, "Polynomial Solution of the Spatial Burmester Problem," *ASME J. Mech. Des.*, **117**, pp. 64–68.
- [25] Su, H.-J., Wampler, C., and McCarthy, J. M., 2004, "Geometric Design of Cylindric PRS Serial Chains," *ASME J. Mech. Des.*, (in press).
- [26] Neilsen, J. and Roth, B., 1995, "Elimination Methods for Spatial Synthesis," *Computational Kinematics*, (eds. J. P. Merlet and B. Ravani), **40**, pp. 51–62, Kluwer Academic Publishers.
- [27] Su, H.-J., and McCarthy, J. M., 2003, "Kinematic Synthesis of a RPS Serial Chains," *Proceedings of the ASME Design Engineering Technical Conference*, September 2–6, 2003, Chicago, IL.
- [28] Kim, H. S., and Tsai, L. W., 2002, "Kinematic Synthesis of Spatial 3-RPS Parallel Manipulators," *Proc. ASME Des. Eng. Tech. Conf.* paper no. DETC2002/MECH-34302, Sept. 29-Oct. 2, 2002, Montreal, Canada.
- [29] Gao, T., Li, T. Y., and Wu, M., 2003, "MixedVol: A Software Package for Mixed Volume Computation," preprint, submitted to *ACM Transactions on Math. Software*, August.
- [30] Su, H.-J., 2004, "Computer Aided Synthesis of Constrained Serial and Parallel Robots," Ph.D. Dissertation, Department of Mechanical and Aerospace Engineering, University of California, Irvine.